JOURNAL OF SOLID STATE CHEMISTRY 33, 17–25 (1980)

X-Ray Photoelectron Spectra of 3*d* Transition Metal Pyrites

H. VAN DER HEIDE, R. HEMMEL, C. F. VAN BRUGGEN, AND C. HAAS

Laboratory of Inorganic Chemistry, Materials Science Center of the University, Nijenborgh 16, 9747 AG Groningen, The Netherlands

Received April 4, 1979

Photoelectron spectra of the synthetic compounds FeS_2, CoS_2, NiS_2, $MnSe_2$, $CoSe_2$, and $NiSe_2$ and of a natural crystal of MnS_2, all with the pyrite structure, are reported. The sulfur 3*s* and selenium 4*s* contributions are split into peaks for bonding and antibonding orbitals due to the covalent bonding in the molecular anion pairs. The difference in lineshape of the peaks for the bonding and antibonding orbitals is attributed to vibronic effects. The metal $2p_{3/2}$ spectra show the effects of multiplet splitting and satellites due to shake-up or shake-off processes. The valence band spectra consist of slightly overlapping contributions of anion *p* and metal 3*d* electrons. The metal 3*d* spectrum of FeS_2 has a single strong peak of width 0.9 eV. The 3*d* spectra of the other compounds show structure due to several final state configurations.

Introduction

Many of the dichalcogenides of the 3*d* transition metals MX_2 (X = S, Se, Te) crystallize in the pyrite structure. This structure is cubic, space group T_h^6 (Pa_3), and can be considered as a NaCl-like grouping of metal atoms and chalcogen atom pairs X_2. The distance in an X_2 pair is short, due to the presence of a covalent bond. Several of the MX_2 compounds with the pyrite structure can be prepared only under high pressure (*1*).

The magnetic and electrical properties of the 3*d* transition metal dichalcogenides with the pyrite structure have been studied in considerable detail, and show a large variety in behavior (*2–9*). Attempts have been made to describe and explain the observed behavior of the pyrites in terms of qualitative energy level schemes or band structure calculations (*1, 10–14*).

In this paper we report a systematic study of the X-ray photoelectron spectra of the 3*d* transition metal dichalcogenides MnS_2, FeS_2, CoS_2, NiS_2, $MnSe_2$, $CoSe_2$, and $NiSe_2$ with the pyrite structure. The valence band spectra of FeS_2 (*15–17*), NiS_2 (*16–18*), CoS_2 (*17*), and ZnS_2 (*18*) have been reported in the literature. We observed the spectra of the core levels, of the bonding and antibonding orbitals of the anion pairs, and of the valence band region consisting of sulfur 3*p* (or selenium 4*p*) and metal 3*d* orbitals. The structure in the spectra of the 3*d* electrons is discussed in terms of a ligand-field description of localized $3d^{n-1}$ final states.

Experimental Procedures

As starting materials the pure elements (Koch–Light) were used; the Mn flakes were etched to remove oxide layers. Polycrystalline samples were prepared by heating stoichiometric amounts of the elements in evacuated quartz ampoules for about 2 weeks. The preparation temperatures for the

0022-4596/80/070017-09$02.00/0

sulfides and selenides were 400 and 700°C, respectively. In order to obtain a homogeneous product, the samples were crushed and heated again at 700°C for 2 weeks. In this way we were able to obtain pure, homogeneous samples of FeS_2, CoS_2, NiS_2, $MnSe_2$, $NiSe_2$, and $CoSe_2$. Single crystals of FeS_2, CoS_2, and NiS_2 were grown by chemical transport in evacuated quartz ampoules, using Cl_2 as a transport agent (*19*). The chlorine pressure in the tube was 0.2–0.3 atm, the temperature gradient about 660–715°C. Single crystals of 2–4 mm were formed at the cold site of the tube.

We have not been able to prepare a good sample of MnS_2; the reported spectra are obtained from a natural single crystal.

The purity and crystal structure of the samples were checked by chemical analysis and X-ray powder diffraction.

Photoelectron spectra were collected on an AEI-ES 200 spectrometer, using Mg$K\alpha$ (energy 1253.6 eV, linewidth $\approx$ 0.8 eV) and Al$K\alpha$ (energy 1486.3 eV, linewidth $\approx$ 1.0 eV) radiation. In some cases (Fig. 8 only) monochromatized Al$K\alpha$ radiation (linewidth $\approx$ 0.35 eV) was used.

The materials to be investigated were handled in a glove box attached to the spectrometer. Indium foil was mounted on the sample holder and cleaned by argon ion etching until all signs of oxidation had vanished. The samples, which were in sealed tubes, were then brought into the glove box. To remove the remaining oxygen and water in the glove box a copper coil was cooled with liquid nitrogen until all signs of condensation had disappeared. The sample tube was then opened and the sample was powdered to obtain a fresh clean surface. The powder was pressed into the indium foil and inserted into the spectrometer. The result of these precautions was that the oxygen 1*s* peaks had a very low intensity. The samples were maintained at a temperature of 10°C during the measurement. The vacuum in the sample chamber was typically 10^{-9} Torr. The binding energies are measured relative to the Fermi energy. Some spectra were taken of powdered samples fixed on adhesive tape, in order to avoid interference with In peaks.

The data were corrected for the analyzer transmission, scattered electrons, and $K\alpha_{3,4}$ satellites using a computer program (*20*).

Core Levels of Anion Pairs

In the pyrites one can clearly distinguish pairs of anions at short distances from one another. Between the anions in such a pair there is a single strong covalent bond. A molecular orbital diagram of an anion pair is given in Fig. 1. The inner core levels 1*s*, 2*s*, 2*p* contribute little to the bonding, due to the small radial extension of these orbitals. The overlap of 3*s* orbitals of the two sulfur atoms leads to a bonding $3s(\sigma_g)$ and an antibonding $3s(\sigma_u^*)$ molecular orbital, both occupied by two electrons. The $3p_z$ orbitals (the line connecting the two sulfur atoms is taken as the *z*-axis) lead to an occupied bonding $3p_z(\sigma_g)$ and an empty $3p_z(\sigma_u^*)$ orbital. The $3p_{x,y}$ orbitals lead to occupied bonding and antibonding Π molecular orbitals. Hybridization causes a mixing of *s* and *p* molecular orbitals of the same symmetry. A molecular orbital scheme of this type has been used for a discussion of the electronic energy levels of ZrS_3 (*21*).

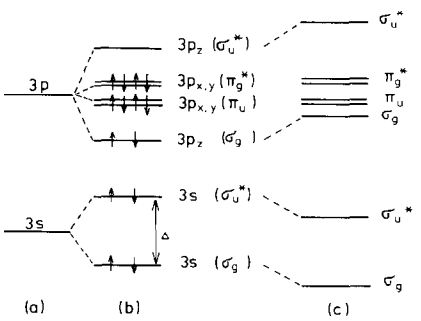

FIG. 1. Molecular orbital diagram of $(S_2)^{2-}$ ion. (a) Atomic energy levels; (b) bonding and antibonding molecular orbitals without *s*–*p* hybridization; (c) with *s*–*p* hybridization.

Experimental results for the core levels of the anion pairs are given in Figs. 2 and 3 and Table I. The spectra of the sulfur $3s$ and selenium $4s$ electrons show the expected splitting Δ between bonding and antibonding molecular orbitals. The magnitude of Δ correlates quite well with the internuclear distance R in the anion pair: for small R the overlap of the $3s$ orbitals of the two sulfur atoms is large, leading to a large value of Δ. The strong dependence of Δ on R causes coupling of $3s$ electrons with vibrations which modulate R.

The observed spectra show a different shape of the $3s(\sigma_g)$ and $3s(\sigma_u^*)$ peaks: the $3s(\sigma_g)$ peak is much broader and has a lower peak height.[1] We attribute this effect to the strong vibronic coupling of the $3s$ hole in the final state with the interatomic vibrations of the anion pair.

The $3s(\sigma_g)$ peak corresponds to a final state with one hole in the bonding molecular orbital. The bonding in this final state will be weaker and the equilibrium internuclear distance will be larger than in the ground state. The $3s(\sigma_u^*)$ final state has a hole in the antibonding molecular orbital. However, the splitting of the bonding and antibonding levels is not symmetric and the antibonding level is probably close to nonbonding due to s–p hybridization (Fig. 1). As a consequence

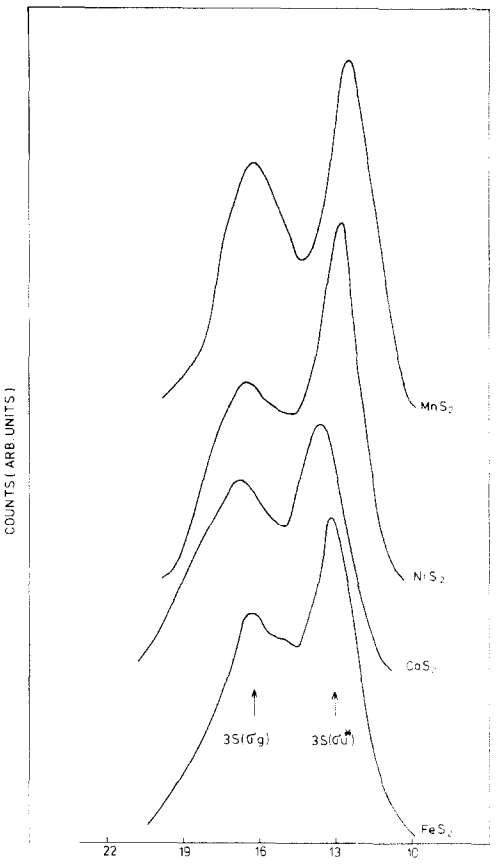

FIG. 2. Photoelectron spectra of sulfur $3s$ electrons in pyrites.

one expects the change of the equilibrium internuclear distance ΔR to be rather small in the $3s(\sigma_u^*)$ final state.

We now consider the effect of vibronic coupling on the lineshape. The XPS phonon linewidth can be calculated using the sudden approximation for the electronic excitation and the Born–Oppenheimer approximation for the electron–phonon interaction (*22–24*). According to the Franck–Condon principle the zero-point and thermal vibrations in the initial state are directly projected into the final state. In the limit of small vibrational quanta and large values of ΔR this leads to a Gaussian lineshape with a width proportional to ΔR. Because ΔR is expected to be

[1] This effect has been observed also in ZrS_3 and $ZrSe_3$, and was ascribed to covalent interactions (*21*). The sulfur $3s(\sigma_g)$ orbitals have nonzero overlap with the metal $4d$, $5s$, and $5p$ orbitals. The $3s(\sigma_u^*)$ orbital in ZrS_3, however, has Π symmetry in the direction of the metal atom due to the "edge-on" coordination of the S_2 group, and can combine only with the $4d$ and $5p$ oribtals of Zr. The band thus formed will be narrower than that due to $3s(\sigma_g)$. In the pyrites, however, each metal atom is surrounded by six anion pairs in such a way that of each pair one atom is much closer to the metal atom than the other. For such an essentially "end-on" coordination one expects overlap of the orbitals of a particular metal atom only with the orbitals of the atom of the pair closest to the metal atom. This leads to equal covalent interactions for $3s(\sigma_g)$ and $3s(\sigma_u^*)$. Therefore this mechanism cannot explain the observed difference of width of the $3s(\sigma_g)$ and $3s(\sigma_u^*)$ peaks in the pyrites.

TABLE I

CORE LEVELS OF ANION PAIRS[a]

Compound	$2p_{1/2}$	$2p_{3/2}$	$\sigma_g(3s)$	$\sigma_u^*(3s)$	Δ (eV)	X–X distance R (Å)
MnS_2	162.9	161.9	16.0	12.4	3.6	2.088
FeS_2	163.4	162.4	16.4	13.3	3.1	2.135
CoS_2	163.7	162.6	16.9	13.6	3.3	2.124
NiS_2	163.7	162.7	16.6	12.9	3.7	2.065
			$\sigma_g(4s)$	$\sigma_u^*(4s)$		
$CoSe_2$			16.7	14.2	2.5	2.435
$NiSe_2$			16.3	14.0	2.3	2.417

[a] Binding energies (eV) are given relative to the Fermi level.

larger for the $3s(\sigma_g)$ than for the $3s(\sigma_u^*)$ final state, one expects a larger vibronic broadening of the $3s(\sigma_g)$ peak, as is observed.

Core Levels of Metal Ions

The photoelectron spectra of the metal $3s$ and $2p_{3/2}$ electrons are given in Figs. 4–7 and Table II. The structure in these spectra is caused by multiplet splitting of the final state and satellites involving excitations of a second electron. The metal $3s$ electrons are subject to the exchange interaction with the spin of the partly filled $3d$ shell (*25–27*). For the high-spin $S=\frac{5}{2}$ Mn^{2+} ion this leads to final states ^5S and ^7S. In the pyrites MnS_2 and $MnSe_2$ we observe indeed a well-resolved

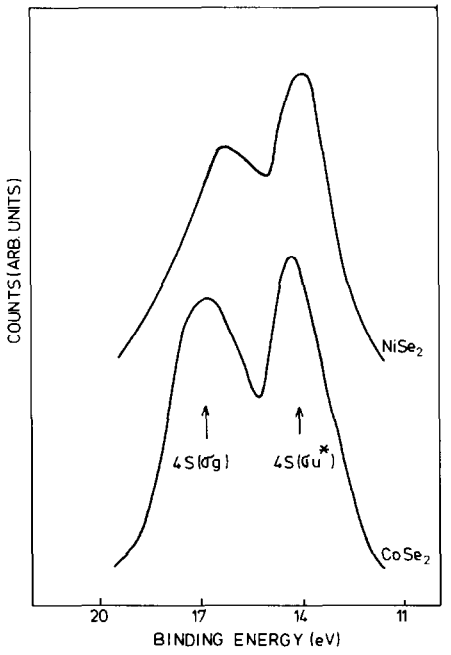

FIG. 3. Photoelectron spectra of selenium $4s$ electrons in pyrites.

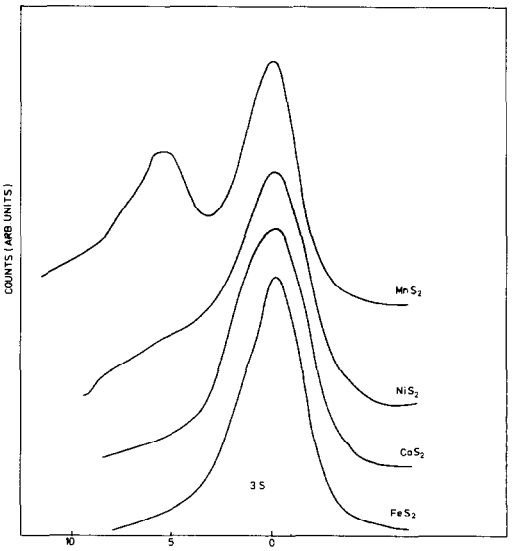

FIG. 4. Photoelectron spectra of metal $3s$ electrons in pyrites. The spectra are shifted so that the maxima of the main peaks coincide.

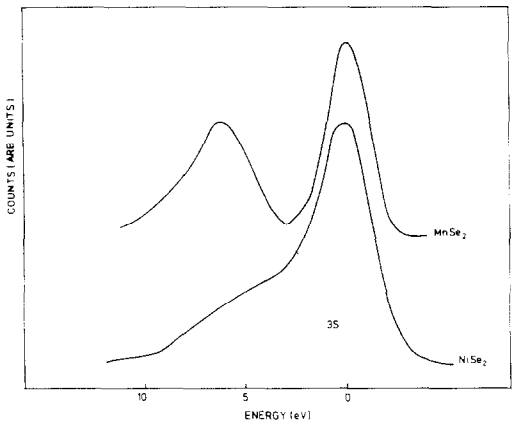

FIG. 5. Photoelectron spectra of metal 3*s* electrons in pyrites. The spectra are shifted so that the maxima of the main peaks coincide.

splitting of the 3*s* spectra of 5.5 and 6.2 eV, respectively. In the other pyrites the exchange splitting is not resolved due to the smaller spin density in the 3*d* shell; the exchange interaction in these cases leads only to a broadening (unresolved splitting) of the 3*s* lines.

Recent calculations showed that the magnitude of the 3*s* splitting is strongly influenced by correlation effects due to the reorganization of the *M* shell electrons in the final 3*s* hole state (*28*). The 3*s* splitting is expected to be proportional to the spin density in the 3*d* shell. Experimental (*26*) and theoretical (*29*) evidence indicates that in the Mn^{2+} compounds the 3*s* splitting decreases with increasing covalency of the metal–ligand bonds. The observed 3*s* splitting of 5.5 and 6.2 eV for MnS_2 and $MnSe_2$ are rather high, if compared with the values of 6.3, 6.0, 4.8, and 6.0 eV, reported for MnF_2, $MnCl_2$, $MnBr_2$ (*26*), and α-MnS (*30*), respectively. Indeed one would expect a smaller splitting for MnS_2 and especially for $MnSe_2$, due to the larger covalency of these compounds as compared with the Mn-halides.

The $2p_{3/2}$ spectra of the pyrites consist of a main line and a weaker secondary maximum at a higher binding energy. The width of the

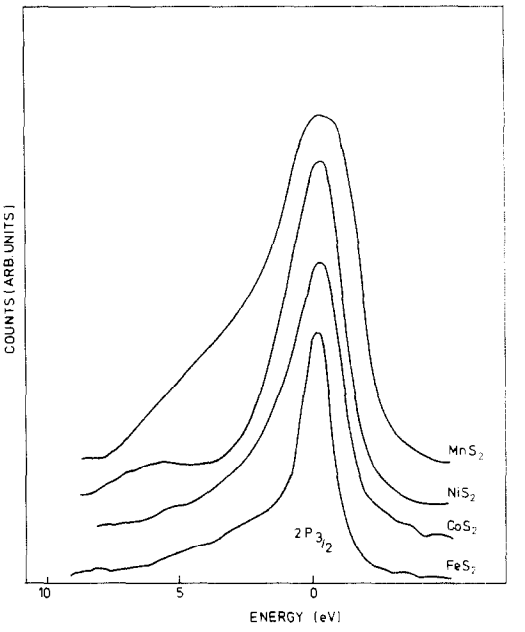

FIG. 6. Photoelectron spectra of metal $2p_{3/2}$ electrons in pyrites. The spectra are shifted so that the maxima of the main peaks coincide.

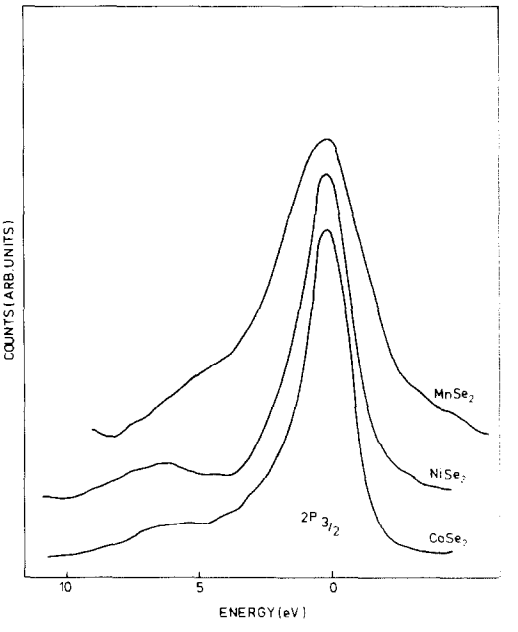

FIG. 7. Photoelectron spectra of metal $2p_{3/2}$ electrons in pyrites. The spectra are shifted so that the maxima of the main peaks coincide.

main line strongly increases in the series FeS_2–CoS_2–NiS_2–MnS_2 and in the series $CoSe_2$–$NiSe_2$–$MnSe_2$ (Table II). The effects of multiplet splitting of the $2p_{3/2}$ are complex due to the possibility of coupling both orbital and spin momentum in the final state (*25, 31, 32*). It was shown that the net effect of multiplet splitting on the main peak of the $2p_{3/2}$ spectrum of Mn^{2+} compounds is an asymmetric broadening at the high-energy side. An asymmetric broadening of this type is observed indeed in the $2p_{3/2}$ spectra of MnS_2 and $MnSe_2$ (Figs. 6 and 7). In FeS_2 the metal ion is in a low-spin $(3d)^6$ $S=0$ configuration, only one final state is possible, and no multiplet splitting is expected. This explains the observed small width of the $2p_{3/2}$ peak of FeS_2. Because of the smaller values of the spin density in the $3d$ shell of the metal ion in CoS_2, $CoSe_2$, NiS_2, and $NiSe_2$ one expects in these compounds a broadening of the main $2p_{3/2}$ peak caused by multiplet splitting smaller than that in the Mn dichalcogenides, as is observed.

Several of the $2p_{3/2}$ spectra show satellites at 5–6 eV higher binding energies. It is remarkable that the $2p_{3/2}$ spectrum of FeS_2 shows no satellite structure. For transition metal compounds the origin of the satellite peaks is a controversial topic. Satellites have been attributed to shake-up transitions of metal $3d \rightarrow 4s$ nature (*33, 34*) or to ligand-orbital to metal-orbital charge transfer (*35–37*). In the Fe, Co, and Ni pyrites the metal $3d(t_{2g})$ orbitals are fully occupied and charge transfer transitions from ligand orbitals are only possible to unoccupied $3d(e_g)$ orbitals. If satellite structure is due to transitions of this type, one expects strong satellites for ions with unoccupied $3d(e_g)$ orbitals, i.e., for FeS_2, NiS_2, CoS_2, and MnS_2. However, only the $2p_{3/2}$ spectra of NiS_2 and $NiSe_2$ (and to a lesser extent that of $CoSe_2$) show pronounced satellites; satellites in the $2p_{3/2}$ spectra of FeS_2, MnS_2, $MnSe_2$, and $CoSe_2$, if at all present, are weak.

It was noticed that satellites do not occur in low-spin diamagnetic compounds (*34*). The absence of satellites in FeS_2 agrees with this rule. Yin *et al.* (*34*) made an attempt to explain this rule and other observed data on satellites in terms of monopole selection rules for metal $3d \rightarrow 4s$ shake-up transitions. However, his approach was criticized by Jörgensen (*38*), and in our opinion no final answer has been given so far to the problem of the origin of $2p_{3/2}$ satellites in transition metal compounds.

TABLE II

CORE LEVELS OF METALS IONS[a]

Compound	$2p_{3/2}$ Binding energy (eV)	$2p_{3/2}$ Width (eV)	$\langle 3s \rangle$ Binding energy (eV)	$\langle 3s \rangle$ Width (eV)
MnS_2	640.4	~4.0	82.6 (^5S) 88.1 (^7S)	
FeS_2	706.7	1.6	92.0	3.5
CoS_2	778.1	2.6	101.9	4.2
NiS_2	853.6	2.7	111.9	4.3
$MnSe_2$	640.5	~4.0	82.6 (^5S) 88.8 (^7S)	
$CoSe_2$	778.3	2.0		
$NiSe_2$	853.2	2.2	112.0	3.6

[a] Binding energies (eV) are given relative to the Fermi level.

Valence Band Spectra

The valence band spectra of the pyrites are shown in Fig. 8. The observed spectra of FeS_2, CoS_2, and NiS_2 agree with spectra previously reported (*15–17*). Some of the valence band spectra have been recorded with and without a monochromator. The noise for spectra with monochromatized radiation is larger due to the lower intensity. The structure in the valence band spectra taken with unmonochromatized radiation is real and reproducible. The valence band spectra consist of contributions of the sulfur $3p$ (selenium $4p$) and metal $3d$ electrons. A

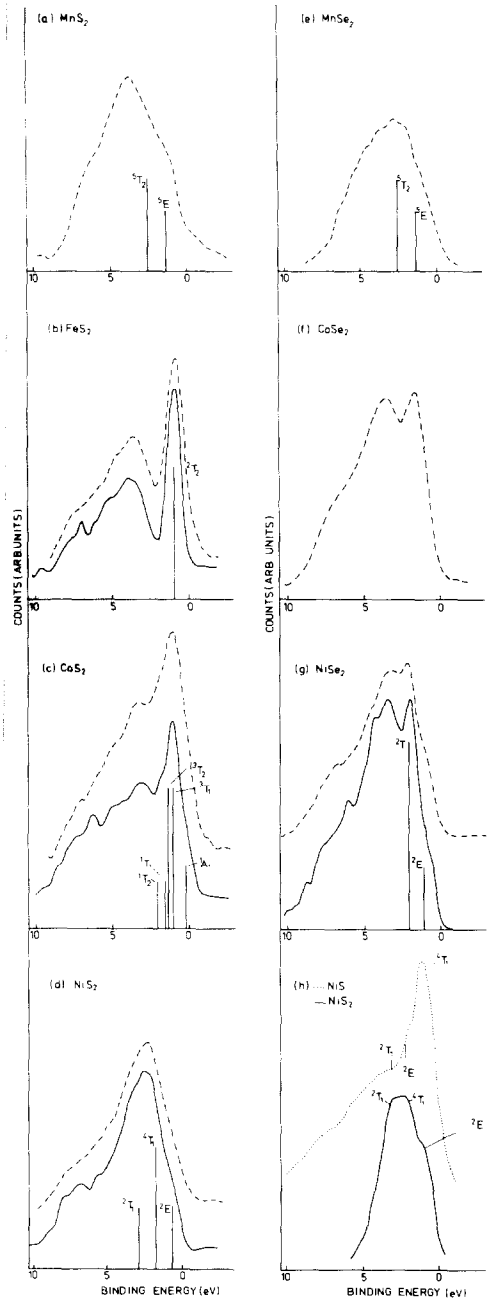

FIG. 8. Valence band spectra of pyrites; spectra marked by solid lines are taken with monochromatized Al$K\alpha$ radiation, those marked by broken lines with unmonochromatized Al$K\alpha$ radiation. Calculated positions (from $10Dq \approx 2.4$ eV, $B \approx 0.06$ eV, and $C = 4B$) and relative intensities of $3d$ peaks are represented by vertical lines. In (h) the $3d$ spectrum of NiS_2 (obtained from (d) by subtracting the S($3p$) spectrum of FeS_2) is compared with the valence band of NiS (dotted line).

comparison of XPS and sulfur $K\beta$ X-ray emission showed directly that in FeS_2, CoS_2, and NiS_2 the contribution of the d electrons lies at the low-binding-energy side of the valence band (*39*).

The contribution of sulfur $3p$ electrons, which are best represented by a band-like description, is probably not very different for the different pyrites. The $3d$ electrons are accounted for by a ligand-field description of localized $3d^{n-1}$ final states of the transition metal ions. A description of this type has been successful for the interpretation of several transition metal compounds (*40–42*). The first coordination sphere of the metal atoms in the pyrite structure is a distorted octahedron of chalcogen atoms. Therefore we expect in first approximation that the interaction with ligands will lead to a ligand-field splitting of octahedral symmetry (O_h). The multiplet splitting then depends only on the Racah parameters, B and C describing the electrostatic repulsion of the d electrons, and the ligand-field parameter $10Dq$ (*43*).

The photoionization of a d electron in FeS_2 (ground state of metal ion $^1A_{1g}(t_{2g})^6$) leads to a single final state $^2T_{2g}(t_{2g})^5$. Therefore the spectrum of $3d$ electrons in FeS_2 is expected to show a single peak. The observed spectrum shows indeed a strong peak, of width 0.9 eV, at the top of the valence band. The structure below this peak is ascribed to broad energy bands, derived from (mainly) sulfur $3p$ orbitals.

The top of the valence band of CoS_2 shows additional structure, because photoionization of the ^2E_g ground state leads to several final states: $^1A_{1g}$, $^3T_{1g}$, $^3T_{2g}$, $^1T_{1g}$, $^1T_{2g}$. For NiS_2 the ground state is $^3A_{2g}$, and the final states are ^2E_g, $^4T_{1g}$, $^2T_{1g}$. The energies and relative intensities, obtained from ligand-field theory (*44*), account reasonably well for the observed structure. However, the data are not accurate enough to permit a determination of crystal-field and Racah parameters. The spectrum of $CoSe_2$ shows no resolved structure.

In Fig. 8h the contribution of the $3d$ electrons of Ni has been obtained by subtracting the sulfur $3p$ valence band obtained from the FeS_2 spectrum where $3p$ and $3d$ bands are clearly separated. The spectrum is rather different from the spectrum of $3d$ electrons in NiS, NiO, NiF_2, and $NiCl_2$ (*42*). This difference is due to the larger crystal-field splitting in NiS_2 which results in a reversal of the peaks due to the ^2E_g and $^4T_{1g}$ final states. As a consequence one expects that the nature of the top of the valence band of NiS_2 is quite different from that of NiS.

The spectrum of $NiSe_2$ differs from that of NiS_2 and shows two $3d$ peaks. However, whereas NiS_2 is an antiferromagnetic semiconductor with well-developed magnetic moments at the Ni atoms (*5*), $NiSe_2$ is a nonmagnetic compound and is presumably best described by a low-spin ground state, $^1A_{1g}(t_{2g}{}^6e_g^2)$. This leads to only two final states, $^2T_{2g}$ and ^2E_g.

For MnS_2 and $MnSe_2$ two final states, ^5E_g and $^5T_{2g}$, are expected. The MnS_2 spectrum shows some evidence of this splitting, but the data are not accurate enough to permit a determination of $10Dq$).[2]

Discussion

In this section we compare the photoelectron spectra with other evidence for the electronic structure.

The variation of the electrical and magnetic properties in the series FeS_2–CoS_2–NiS_2–CuS_2 has been ascribed to the increasing number of electrons in the narrow $3d(e_g^*)$ band (*1, 13*). In this model the $3d$ levels of the metal are split by the ligand field in a set of $3d(t_{2g})$ orbitals, which are (almost) nonbonding and form a narrow band, and a set of $3d(e_g^*)$ orbitals forming an antibonding band. In the semiconductor FeS_2 the $3d(t_{2g})$ band is occupied and the $3d(e_g^*)$ is empty From photoelectron spectra we find the width of the $3d(t_{2g})$ band to be about 0.9 eV (width of the observed band including the instrumental linewidth).

The photoelectron spectra of FeS_2 and NiS_2 have been compared with spin-polarized SCF-Xα cluster calculations on octahedral $FeS_6{}^{10-}$ and $NiS_6{}^{10-}$ clusters (*16*) However, these calculations do not take into account the presence of $(S_2)^{2-}$ moleculear anions and have neither the proper geometry nor the proper charge at the sulfur atom. The energy levels of these calculations are relevant for FeS and NiS, not for FeS_2 and NiS_2.

The only available calculation of the band structure of the pyrites employs a LCAO method to obtain the energy bands of FeS_2 (*12*). This calculation leads to narrow energy bands t_{2g} and e_g for the $3d$ orbitals, in agreement with the experimental data. However, the calculations also lead to narrow Π_u and σ_g for the bonding sulfur $3p$ orbitals. This is not in agreement with the observed photoelectron spectrum which shows a broad band (width about 6 eV) for the sulfur $3p$ orbitals.

[2] The valence band of MnS_2 is very similar to that of MnS (*45*). A comparison of the valence band of MnS with that of MgS indicates the assignment of shoulders at 1.5 and 2.5 eV to $3d^4$ final states ^5E_g and $^5T_{2g}$.

Acknowledgments

We thank Professor Perdok, Laboratory of Solid State Physics, Groningen, for kindly putting at our disposal a single crystal of MnS_2, and Professor F. Jellinek and Dr. G. Sawatzky for helpful discussions.

References

1. T. A. BITHER, R. J. BOUCHARD, W. H. CLOUD, P. O. DONOHUE, AND W. J. SIEMONS, *Inorg. Chem.* **7**, 2208 (1968).
2. G. BROSTINGEN AND A. KJEKSHUS, *Acta Chem. Scand.* **24**, 2993 (1970).
3. S. FUDUSETH AND A. KJEKSHUS, *Acta Chem Scand.* **23**, 2325 (1969).
4. H. S. JARRETT, W. H. CLOUD, R. J. BOUCHARD, S. R. BUTLER, C. G. FREDERICK, AND G. L. GILSON, *Phys. Rev. Lett.* **21**, 617 (1968).
5. K. ADACHI, K. SATO, AND M. TAKEDA, *J. Phys. Soc. Japan* **26**, 631 (1969).

6. S. OGAWA, S. WAKI, AND T. TERANISHI, *Int. J. Magn.* **5**, 349 (1974).
7. S. MARCUS AND T. A. BITHER, *Phys. Lett. A* **32**, 363 (1970).
8. K. ADACHI, K. SATO, M. MATSUURA, AND M. OHASHI, *J. Phys. Soc. Japan* **29**, 323 (1970).
9. P. PANISSOD, G. KRILL, M. LAHRICHI, AND M. F. LAPIERRE, *Phys. Lett. A.* **59**, 221 (1971).
10. J. B. GOODENOUGH, *J. Solid State Chem.* **5**, 144 (1972).
11. F. GAUTIER, G. KRILL, M. F. LAPIERRE, P. PANISSOD, C. ROBERT, G. CZJEK, J. FINK, AND H. SCHMIDT, *Phys. Lett. A* **53**, 31 (1975).
12. M. A. KHAN, *J. Phys. C* **9**, 81 (1976).
13. A. SCHLEGEL AND P. WACHTER, *J. Phys. C* **9**, 3363 (1976).
14. J. A. WILSON AND G. D. PITT, *Phil. Mag.* **23**, 1297 (1971).
15. U. BERG, G. DRÄGER, K. MOSEBACH, AND O. BRÜMMER, *Phys. Status Solidi B* **75**, K89 (1976).
16. E. K. LI, K. H. JOHNSON, D. E. EASTMAN, AND J. L. FREEOUF, *Phys. Rev. Lett.* **32**, 470 (1974).
17. A. OHSAWA, H. YAMAMOTO, AND H. WATANABE, *J. Phys. Soc. Japan* **37**, 568 (1974).
18. H. YAMAMOTO, T. NAKAGAWA, H. ODONERA, AND H. WATANABE, *J. Phys. Soc. Japan* **43**, 1095 (1977).
19. R. J. BOUCHARD, *J. Cryst. Growth* **2**, 40 (1968).
20. E. ANTONIDES, Thesis, Groningen (1977).
21. F. JELLINEK, R. A. POLLACK, AND M. W. SHÄFER, *Mater. Res. Bull.* **9**, 845 (1974).
22. K. HUANG AND A. RHYS, *Proc. Roy. Soc. London Ser. A* **208**, 352 (1951).
23. M. WAGNER, *J. Chem. Phys.* **41**, 3939 (1964).
24. P. H. CITRIN, P. EISENBERGER, AND D. R. HAMANN, *Phys. Rev. Lett.* **33**, 965 (1974).
25. C. S. FADLEY AND D. A. SHIRLEY, *Phys. Rev. A* **2**, 1109 (1970).
26. J. C. CARVER, C. K. SCHWEITZER, AND T. A. CARLSON, *J. Chem. Phys.* **57**, 973 (1972).
27. S. P. KOWALCZYK, L. LEY, R. A. POLLACK, F. R. MCFEELY, AND D. A. SHIRLEY, *Phys. Rev. B* **7**, 4009 (1973).
28. P. S. BAGUS, A. J. FREEMAN, AND F. SASAKI, *Phys. Rev. Lett.* **30**, 850 (1973).
29. E. K. VIINIKKA AND S. LARSSON, *J. Electron Spectr.* **7**, 163 (1975).
30. H. H. HEIKENS, Thesis, Groningen (1977).
31. R. P. GUPTA AND S. K. SEN, *Phys. Rev. B* **10**, 71 (1974).
32. T. A. CARLSON, J. C. CARVER, AND G. A. VERNON, *J. Chem. Phys.* **62**, 932 (1975).
33. A. ROSENCWAIG, G. K. WERTHEIM, AND H. J. GÜGGENHEIM, *Phys. Rev. Lett.* **27**, 479 (1971).
34. L. YIN, I. ADLER, T. TSANG, L. J. MATIENZO, AND S. O. GRIM, *Chem. Phys. Lett.* **24**, 81 (1974).
35. K. S. KIM, *J. Electron Spectr.* **3**, 217 (1974).
36. M. BRISK AND A. D. BAKER, *J. Electron Spectr.* **7**, 197 (1975).
37. G. A. VERNON, G. STUCKY, AND T. A. CARLSON, *Inorg. Chem.* **15**, 278 (1976).
38. C. K. JÖRGENSEN, *Struct. Bonding* **24**, 1 (1975).
39. C. SUGIURA, I. SUZUKI, J. KASHIWAKURA, AND Y. GOHSHI, *J. Phys. Soc. Japan* **40**, 1720 (1976).
40. G. K. WERTHEIM, H. J. GÜGGENHEIM, AND S. HÜFNER, *Phys. Rev. Lett.* **30**, 1050 (1973).
41. D. E. EASTMAN AND J. L. FREEOUF, *Phys. Rev. Lett.* **34**, 395 (1975).
42. S. HÜFNER AND G. K. WERTHEIM, *Phys. Rev. B* **8**, 4857 (1973).
43. S. SUGANO, Y. TANABE, AND M. KAMIMURA, "Multiplet of Transition Metal Ions in Crystals," Academic Press, New York (1970).
44. P. A. COX, *Struct. Bonding* **24**, 59 (1975).
45. H. H. HEIKENS, C. F. VAN BRUGGEN, AND C. HAAS, *J. Phys. Chem. Solids* **39**, 833 (1978).